HIM-10 Is Required for Kinetochore Structure and Function on *Caenorhabditis elegans* Holocentric Chromosomes

Mary Howe,* Kent L. McDonald,‡ Donna G. Albertson,§ and Barbara J. Meyer*

*Howard Hughes Medical Institute, Department of Molecular and Cell Biology, and ‡Electron Microscope Laboratory, University of California, Berkeley, Berkeley, California 94720; and §Cancer Research Institute, University of California, San Francisco, San Francisco, California 94143

Abstract. Macromolecular structures called kinetochores attach and move chromosomes within the spindle during chromosome segregation. Using electron microscopy, we identified a structure on the holocentric mitotic and meiotic chromosomes of *Caenorhabditis elegans* that resembles the mammalian kinetochore. This structure faces the poles on mitotic chromosomes but encircles meiotic chromosomes. Worm kinetochores require the evolutionarily conserved HIM-10 protein for their structure and function. HIM-10 localizes to the kinetochores and mediates attachment of chromosomes to the spindle. Depletion of HIM-10 disrupts kinetochore structure, causes a failure of bipolar spindle attachment, and results in chromosome nondisjunction. HIM-10 is related to the Nuf2 kinetochore proteins conserved from yeast to humans. Thus, the extended kinetochores characteristic of *C. elegans* holocentric chromosomes provide a guide to the structure, molecular architecture, and function of conventional kinetochores.

Key words: kinetochore • holocentric chromosomes • mitosis • meiosis • *Caenorhabditis elegans*

Introduction

When cells divide, the replicated sister chromatids must partition equally and with high fidelity to daughter cells. At the onset of mitosis, chromosomes condense and microtubules form a bipolar spindle, with a microtubule nucleation center at each end. Faithful chromosome segregation requires that sister chromatids capture microtubules emanating from opposite spindle poles. Paired chromatids then align at the spindle equator (the metaphase plate) through oscillatory movements directed toward and away from the poles. Once alignment is complete, sister chromatids separate from each other and segregate to opposite poles during anaphase (Nicklas, 1997). Establishing bipolar spindle attachment and alignment of chromosomes at metaphase is thus a primary event that ensures daughter cells will receive an identical complement of chromosomes.

Chromosomes capture microtubule plus ends via kinetochores. The kinetochore is a complex and dynamic macromolecular structure that assembles at a region of each chromosome termed the centromere and moves chromosomes within the spindle. Much of chromosome movement is driven by the coordinated activities of microtubule-based motor proteins at the kinetochore coupled to microtubule polymerization and depolymerization (Heald, 2000; Sharp et al., 2000b). In addition to promoting chromosome movement and alignment during prometaphase, kinetochores drive chromosome poleward motion during anaphase, and they control when this force is exerted. Kinetochores also regulate the transition from metaphase to anaphase by inhibiting chromatid separation until all chromatids are properly attached and aligned (Amon, 1999; Shah and Cleveland, 2000).

Molecules that localize to centromere/kinetochore regions can be classified in part by their functional roles (Maney et al., 2000): proteins that localize constitutively and recruit other components (e.g., CENP-A, the centromere-specific histone H3 variant) (Howman et al., 2000); proteins that anchor kinetochores to spindles (e.g., CENP-E, a kinesin-like protein) (Lombillo et al., 1995); motor proteins that generate chromosome movement towards the poles (e.g., cytoplasmic dynein) (Savoian et al., 2000; Sharp et al., 2000a); and checkpoint proteins that participate in a sensory mechanism functioning to delay the onset of anaphase until proper attachment and alignment has occurred (e.g., MAD and BUB) (Amon, 1999; Shah and Cleveland, 2000).

The known kinetochore proteins fail to fully explain kinetochore behaviors. For example, how are kinetochores assembled and attached to spindles? To define additional proteins important for kinetochore assembly and for stable bipolar spindle attachment, we turned to *Caenorhabdi-*

Address correspondence to Barbara J. Meyer, Howard Hughes Medical Institute, Department of Molecular and Cell Biology, 401 Barker Hall, University of California, Berkeley, Berkeley, CA 94720-3204. Tel.: (510) 643-5585. Fax: (510) 643-5584. E-mail: bjmeyer@uclink4.berkeley.edu

tis elegans because the unusual structure of its chromosomes provides a unique opportunity to identify these molecules. In contrast to the monocentric chromosomes of yeast and vertebrates, which have highly localized centromeres and discrete sites for kinetochore assembly, the holocentric chromosomes of *C. elegans* have centromeric activity, kinetochore structures, and sites of microtubule attachment dispersed along the chromosome length (Albertson and Thomson, 1982). Unlike acentric fragments of monocentric chromosomes, fragments of holocentric chromosomes (free duplications) can segregate, but with reduced fidelity, presumably because they retain kinetochore activity but have fewer microtubule attachments than whole chromosomes (Albertson and Thomson, 1982). These free duplications are expected to be more sensitive to the disruption of chromosome–spindle interactions than whole chromosomes, and partial loss-of-function mutations in genes encoding kinetochore proteins might increase free duplication loss without causing death from disruption of whole chromosome segregation.

In this study, we analyzed the *him-10* (high incidence of males) gene of *C. elegans*. Reduction of *him-10* activity decreases the stability of free duplications during mitosis (Hedgecock and Herman, 1995) and increases the frequency of X chromosome nondisjunction (Hodgkin et al., 1979). We show that HIM-10 is an evolutionarily conserved kinetochore component that is essential in *C. elegans* for chromosome segregation during mitosis and meiosis. Depletion of HIM-10 disrupts the kinetochore structure defined by EM, resulting in failure of bipolar spindle attachment. Thus, HIM-10 is essential for the assembly or integrity of the kinetochore.

Materials and Methods

Mapping him-10

him-10 had been localized to the 2–map unit interval between *dpy-17* and *unc-32* on chromosome III. Three-factor mapping placed *him-10* between *lon-1* and *sma-3*, very close to *sma-4*: 36/51 Sma non-Lon recombinants from *lon-1 sma-3/him-10* heterozygotes, 15/15 Sma non-Lon recombinants from *lon-1 sma-4/him-10* heterozygotes, and 25/25 uncoordinated (Unc)[1] non-Sma recombinants from *sma-4 unc-36/him-10* heterozygotes segregated *him-10* mutants; 11/11 Sma non-Unc recombinants from *sma-4 unc-36/him-10* heterozygotes, 3/5 Dpy non-Df recombinants from *dpy-17 sDf127 unc-32/him-10* heterozygotes, and 2/28 Unc non-Df recombinants from *dpy-17 sDf121 unc-32/him-10* heterozygotes failed to segregate *him-10* mutants.

Transgenic Animals

Germline transformation experiments were performed (Mello and Fire, 1995) by coinjecting test DNA (20 μg/ml) and marker DNA (roller phenotype) (pRF6, 100 μg/ml) into *him-10(e1511*ts)*/lon-1 sma-4* heterozygotes. Embryos were cultured from each independent homozygous *him-10* transgenic line at the nonpermissive temperature (25°C), and 20 of the resulting Rol and non-Rol adults were scored for rescue of sterility. In transgenic lines that conferred rescue, 31–72% of Rol animals were fertile, whereas <5% of non-Rol animals were fertile.

RNA Interference

A plasmid (YK428) that encodes HIM-10 (sequence data available at EMBL/GenBank/DDBJ under accession no. U00066) was excised from cDNA phagemid yk428e9 (provided by Y. Kohara, National Institute of

---

[1]*Abbreviations used in this paper:* FS, freeze substitution; HPF, high pressure freezing; RNAi, RNA-mediated interference; Unc, uncoordinated.

Genetics, Mishima, Japan). An EcoRI/KpnI fragment including the entire *him-10* ORF was inserted into the doubleT7script2 vector (provided by A. Fire, Carnegie Institution of Washington, Baltimore, MD) to create pMZ6. Plasmid pMZ6 was linearized with either Asp718 or EcoR1 and was used as template for separate Ribomax (Promega) T7 transcription reactions to generate the sense and anti-sense RNA strands. RNAs were annealed (Fire et al., 1998) and diluted to a concentration of 1 or 2 mg/ml for injection into wild-type hermaphrodites.

Antibody Preparation

A SacI/KpnI DNA fragment from YK428 that encodes HIM-10 amino acids 262–491 was cloned into the SacI/KpnI–digested pRSET A expression vector to create plasmid pMZ5, which encodes a 6xHis fusion protein of HIM-10 and an additional 36 amino acids. The fusion protein was purified by Ni-chelate chromatography and used to raise rabbit and rat antisera. Antibodies were affinity purified using Affi-gel 15 resin covalently coupled to the HIM-10 fusion protein (Harlow and Lane, 1988). The affinity-purified antibodies, but not the preimmune sera, identified a single ~69-kD protein in Western blots to embryonic extracts (provided by K. Hagstrom, Howard Hughes Medical Institute) (Fig. 1 C).

Antibody Staining

The antibody staining protocol was devised by A. Chan (Howard Hughes Medical Institute). Adult worms were dissected into sperm salts (50 mM Pipes, pH 7, 25 mM KCl, 1 mM MgSO₄, 45 mM NaCl, and 2 mM CaCl₂) on a slide, an equal volume of 3% paraformaldehyde (Electron Microscopy Sciences) was added, and the slide was incubated in a humid chamber for 5 min. The slide was freeze cracked on dry ice, placed into 95% ethanol for 1 min, and washed with PBST (1× PBS, 0.5% Triton X-100, and 1 mM EDTA, pH 8). The slide was then incubated with primary antibody overnight and secondary antibody for 5 h, stained with DAPI (10 μg/ml), mounted with DABCO (0.1 g/ml DABCO in 1× PBS and 90% glycerin), and visualized with a Leica TCS NT confocal microscope. The staining patterns shown are representative of the >50 scored wild-type embryos or germ cells. Mouse tubulin antibody directed against sea urchin α-tubulin was a gift from D. Asai (Purdue University, West Lafayette, IN).

EM

Adult worms containing embryos were prepared for EM by high pressure freezing (HPF) followed by freeze substitution (FS) as described previously (McDonald, 1999; Rappleye et al., 1999). Serial longitudinal sections were cut through whole worms containing many embryos and picked up on slot grids. Sections 70 nm thick were cut to visualize the ribosome-free zone at low and medium magnifications, and 50-nm sections were cut to visualize spindle microtubules in longitudinal section at high magnification. In wild-type embryos, we observed the ribosome-free zone in several hundred sections representing >20 different spindles at late prometaphase/metaphase. For several spindles, complete serial section series were photographed. For RNA-mediated interference (RNAi)–treated embryos, it was more difficult to identify the stages of mitosis, but again we looked at several hundred sections representing ~10 different cells with condensed chromatin, and the ribosome-free zone was not apparent. One spindle from an RNAi-treated embryo was followed through all serial sections.

Fluorescence In Situ Hybridization

A 950-bp repeat from the 5S rDNA locus on chromosome V was amplified from genomic DNA using PCR with primers 5SrDNA1 (5′-TACTTGGATCGGAGACGGCC-3′) and 5SrDNA2 (5′-CTAACTGGACTCAACGTTGC-3′). The purified PCR fragment was used as template in a nick translation reaction (Albertson and Thomson, 1993) that incorporated Alexa Fluor 568-5-dUTP (Molecular Probes) to generate the 5S rDNA probe (provided by T. Wu, Howard Hughes Medical Institute). *C. elegans* embryos were fixed with 2% paraformaldehyde and permeabilized by freeze cracking on dry ice, followed by exposure to (−20°C) 95% ethanol, and returned to room temperature. The embryos were rehydrated and hybridized to the fluorescent probe as described previously (Dernburg and Sedat, 1998) and visualized with a confocal microscope.

Scoring FISH Embryos

Each embryo was subjected to serial optical sectioning with ~1.5-fold sampling in the z axis. Images of the DAPI and Alexa-Fluor serial sections

were merged using the Leica TCS NT software. Each z-series through an embryo was analyzed section by section to follow individual nuclei and count the total number of independent FISH signals (5S rDNA loci) within each nucleus. Ambiguity in the number of FISH signals in a nucleus was treated by recording all probable numbers of signals.

Data Analysis

The mode of the distribution of chromosomes in each cell was used to characterize the typical number of chromosomes in the nuclei of a particular embryo. Fisher's exact test was used to compare the proportions of embryos with a normal mode in the control and treatment groups.

The following model was used to compute the rate of abnormal chromosome segregation: if X is the number of cells in an embryo after i cell divisions, then

$$X = 2^i. \tag{1}$$

If C is the probability that a chromosome segregates properly in a single cell division, and Y is the number of cells with nuclei in the mode of the embryo, then

$$Y = (2C)^i. \tag{2}$$

Solving Eq. 1 for i, substituting into Eq. 2, and taking logs of both sides gives

$$\log (Y) = B \log (X), \tag{3}$$

where

$$B = \log (2C)/\log (2). \tag{4}$$

Linear regression was used to estimate B. Then equation 4 was used to recover C. Analysis of variance was used on the model as expressed in Eq. 3 to test whether the parameters were different in the control and treatment groups.

For the calculation of C values in Fig. 2 D and Fig. 6 O, nuclei with an ambiguous number of FISH signals were assumed to be in the mode. However, for the statistical analysis, the ambiguous nuclei were put in the least favorable category. For example, for the control embryos of the RNAi experiment, ambiguous nuclei were assumed to be out of the mode, but for the RNAi-treated embryos, ambiguous nuclei were assumed to be in the mode.

Results

HIM-10 Is Structurally Related to a Kinetochore Protein Conserved from Yeast to Humans

The *him-10* gene was cloned with DNA transformation rescue experiments once *him-10* was mapped very near to the cloned gene *sma-4* (Fig. 1 A). Consistent with this map position, two overlapping cosmids known to encode *sma-4* (W03A3 and R12B2) rescued the temperature-sensitive sterile phenotype of *him-10(e1511*ts*)*, but an adjacent cosmid (F43E9) did not. Analysis of three W03A3 deletion derivatives narrowed the rescuing activity to a single ORF, R12B2.4 (Fig. 1 A). Sequence analysis of a complete *him-10* cDNA clone confirmed the ORF predicted by the *C. elegans* Genome Consortium. *him-10* spans 1.2 kb, includes six exons, and is predicted to encode a protein of 491 amino acids (Fig. 1 B). Comparison of genomic DNA sequence from wild-type and *him-10(e1511*ts*)* animals revealed a single nucleotide change predicted to cause a substitution of serine for proline at amino acid 109. Together, the transformation rescue and the molecular identification

of the *him-10(e1511*ts*)* lesion proved that R12B2.4 encodes HIM-10.

HIM-10 is a conserved coiled coil protein structurally related to the Nuf2 kinetochore proteins of *Schizosaccharomyces pombe, Saccharomyces cerevisiae,* and *Homo sapiens* (Wigge and Kilmartin, 2001). All four proteins have a similar size and prominent coiled coil regions between amino acids 120–350. A stretch of high similarity (amino acids 90–131 of HIM-10) resides outside the coiled coil regions and a short stretch of amino acid identity (SPE-LK, amino acids 245–250) resides within the coiled coil regions. Mutations that alter conserved amino acids have been identified in both stretches, a P109S substitution associated with *him-10(e1511*ts*)* and a L246P substitution in the SPE-LK region associated with *nuf2-3* of *S. pombe* (Nabetani et al., 2001).

Mitotic Chromosome Segregation Is Disrupted in Germ Cells with Reduced him-10 Activity

To assess HIM-10 function, we asked whether the fidelity of mitotic chromosome segregation had been reduced in *him-10(e1511*ts*)* mutants raised at the restrictive temperature (25°C) from embryogenesis through adulthood. ~87% of embryos (n = 2,287) were viable, and all examined had morphologically normal metaphase and anaphase structures. Larvae and adults were not Unc, a phenotype correlated with aberrant mitotic chromosome segregation in somatic cells (O'Connell et al., 1998). However, the adults produced only dead embryos. The oocytes of these adults had an atypical number of bivalents, either larger or smaller than the normal number of six (Fig. 1, D–F; and A. Villeneuve, unpublished results cited in Albertson et al., 1997). Since oocytes arrest in meiotic prophase, before the meiotic divisions (Kimble and White, 1981), the aberrant chromosome number must have resulted from defective mitotic chromosome segregation in the germline. Thus, *him-10* is required for mitotic chromosome segregation in the proliferating germline.

Mitotic Chromosome Segregation Is Disrupted in Embryos Lacking him-10 Activity

The lack of mitotic defects in somatic cells of *him-10*(ts) mutants prompted us to use RNAi to achieve a more potent inhibition of *him-10* function (Fire et al., 1998). Double-stranded RNA corresponding to the entire *him-10*–coding region was injected into the gonads of wild-type adult hermaphrodites, and their progeny were examined. Progeny laid 10–15 h after injection (n = 329) exhibited a range of mutant phenotypes: the majority arrested as embryos or larvae (70%), and others developed into Unc (6%), sterile (1%), or sterile Unc (15%) adults, phenotypes typical of mutants with aberrant chromosome segregation during somatic cell divisions (O'Connell et al., 1998). Only 8% of the progeny appeared wild type. Of the progeny laid 25–35 h after injection (n = 1,546), 97% arrested as embryos or larvae. Two findings suggest that these phenotypes were not caused by aberrant germ cell chromosome segregation. Ooctyes examined 35 h after RNAi treatment had a wild-type number of chromosomes, implying normal germ cell mitosis. In addition, none of the injected hermaphrodites produced males, which would
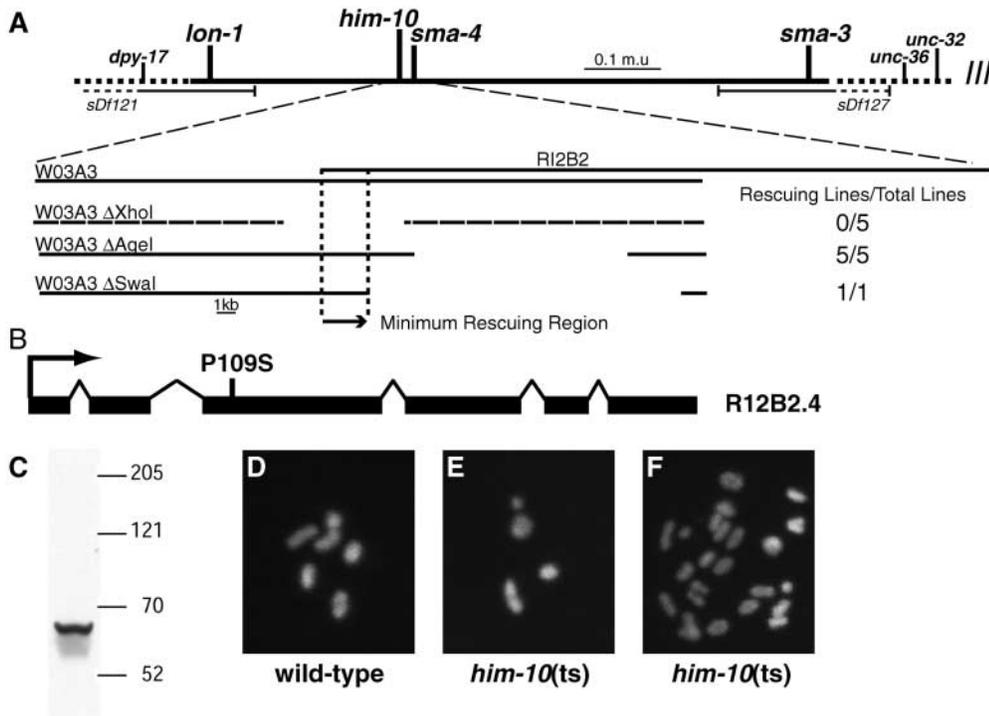
Figure 1. *him-10* encodes a conserved coiled coil protein. (A) A genetic map of the *him-10* region, with an expanded view of molecular clones within the *him*-10 to *sma-4* interval. Two cosmids encoding *sma-4* (R12B2 and W03A3) and W03A3 derivatives that encode the R12B2.4 ORF rescued the sterility of *him-10(e1511ts)*. The number of independent transgenic lines tested for each derivative and the number of lines that rescued the *him-10* phenotype are indicted to the right. (B) The exon/intron structure of the R12B2.4 ORF and the P109S substitution caused by *him-10(e1511*ts) is shown. HIM-10 encodes a homologue of the conserved Nuf2 kinetochore protein. (C) A Western blot of whole worm embryo extract probed with anti–HIM-10 antibody reveals a single band of reactivity that migrated at ∼69 kD. (D–F) Projections of confocal z-series taken of DAPI-stained oocyte diakinesis nuclei from animals raised at 25°C show the mitotic defect rescued above. (D) Wild-type nucleus with a normal set of six bivalents. (E) *him-10*(ts) mutant nucleus with three bivalents and one univalent. (F) *him-10*(ts) mutant nucleus with 22 bivalents and two univalents.

have resulted from nondisjunction events in germ cell mitosis or meiosis (Hodgkin et al., 1979).

Somatic mitotic chromosome segregation was assessed in embryos laid 24 h after the RNAi treatment by determining the segregation pattern of a single chromosome using FISH with a probe to the 5S rDNA locus on chromosome V (Fig. 2, A–C). The number of chromosome V copies was determined for all nuclei in an embryo, and for each embryo, a mode was determined to reflect the most frequent class of nuclei within the embryo. Nuclei were then categorized as being in the mode of the embryo or out of the mode. This analysis allows one to distinguish between mitotic and meiotic chromosome segregation defects. Embryos with normal segregation of chromosome V are expected to have a mode of two (indicative of wild-type meiosis), with all their nuclei in the mode (indicative of wild-type mitosis). Embryos with aberrant mitotic chromosome segregation are expected to have a heterogeneous population of nuclei with many nuclei out of the mode. Nuclei could have zero to one copies (from chromosome loss or nondisjunction), three copies (from nondisjunction), or multiple copies (from repeated nondisjunction or endoreplication) of chromosome V. Embryos with normal mitosis but derived from meiosis-defective germ cells are expected to have a homogenous population of nuclei with a mode other than two. Finally, mitosis-defective embryos derived from meiosis-defective germ cells are expected to have a mode other than 2 and a heterogeneous population of nuclei.

As expected, 13 of 13 untreated embryos had a mode of two, with virtually all nuclei in the mode (Fig. 2 B). By contrast, 12 of 19 RNAi-treated embryos had a heterogeneous population of nuclei, indicating aberrant mitotic chromosome segregation during embryogenesis (Fig. 2 C). Sister nuclei with a three-to-one segregation of chromosome V, a hallmark of nondisjunction, were readily seen in RNAi-treated embryos (Fig. 2 C, arrows). 7 of 19 treated embryos, all under 15 cells, were essentially wild type, potentially because too few cell divisions had taken place for the mitotic defect to have occurred.

Using the model described in the Materials and Methods, we calculated the probability of correct chromosome V segregation (C) for wild-type and RNAi-treated embryos based on the data in the graph of Fig. 2 D. The C value for wild-type embryos was 0.99, indicating that incorrect segregation of chromosome V was rare. The C value for treated embryos was 0.86, indicating that chromosome V segregated incorrectly in 14% of the mitotic divisions. Even with the most conservative treatment of the data, the RNAi-treated group had a significantly higher rate of abnormal cell divisions (p-value ≤ 0.01). Since *C. elegans* has six chromosomes, the probability that approximately one of the chromosomes would segregate abnormally during each cell cycle in the RNAi-treated embryos is 60%, as calculated by $1 − (0.86)^6$. We therefore conclude that *him-10* is essential for faithful chromosome segregation in somatic cells.

Abnormal Mitotic Structures in him-10–deficient Embryos Imply a Defect in Spindle Attachment to Chromosomes

Cytological defects caused by loss of *him-10* activity were readily apparent in RNAi-treated embryos stained with a DNA-intercalating dye (DAPI) and antitubulin antibodies. Mutant embryos had grossly abnormal interphase nu-
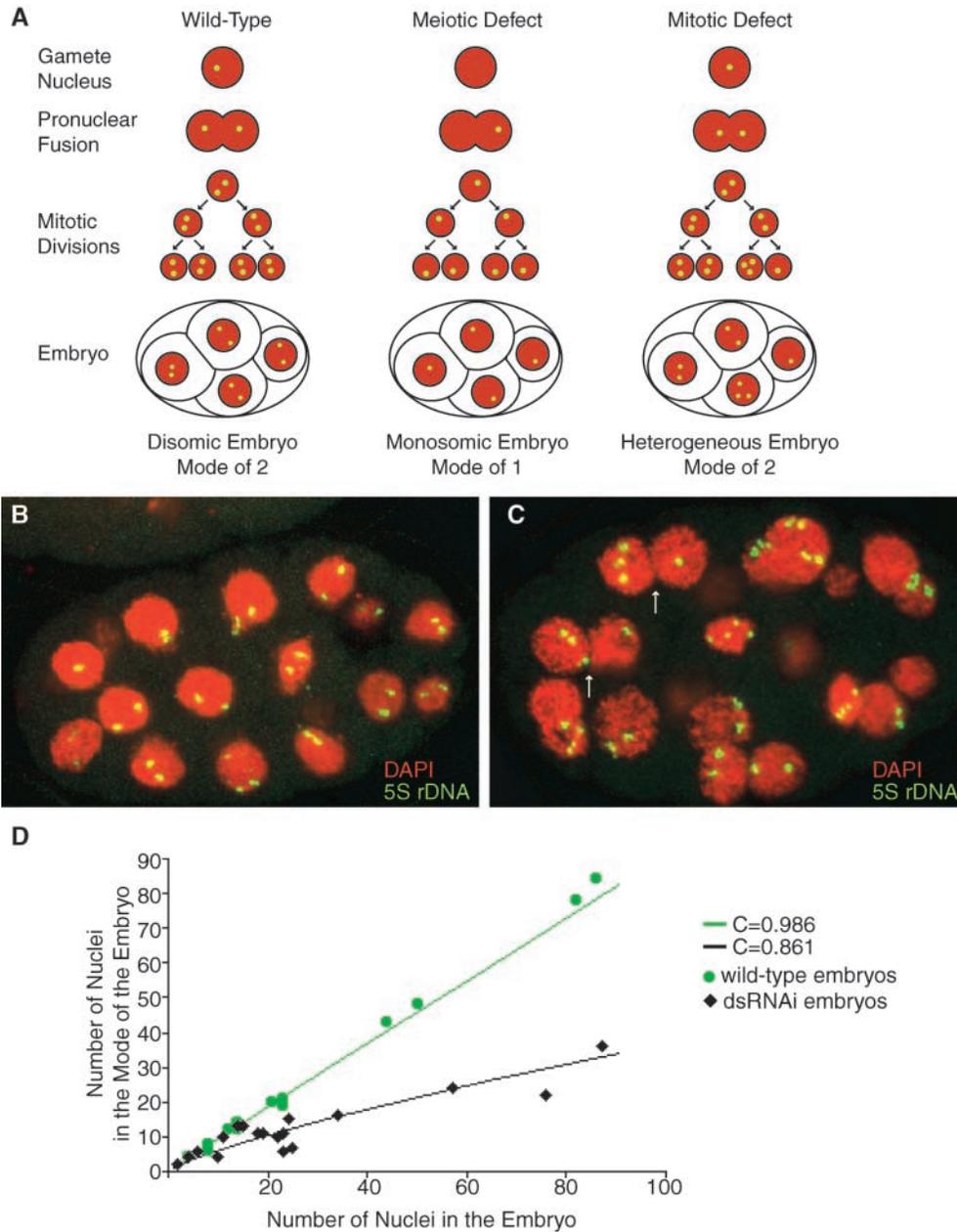
Figure 2. *him-10*(RNAi) embryos exhibit nondisjunction and decreased fidelity of mitotic chromosome segregation. (A) Cartoon of a FISH experiment with a single chromosome probe depicts the outcomes expected from chromosome segregation defects in meiosis or mitosis. Wild-type animals have haploid gametes, diploid zygotes, and uniformly diploid nuclei after several rounds of embryonic cell division. A meiotic defect causes aneuploid gametes and zygotes and uniformly aneuploid embryonic nuclei. Embryos with a mitotic defect have a heterogeneous population of nuclei after several rounds of cell division. Depicted is a nondisjunction event leading to 3-1 chromosome segregation. (B and C) FISH analysis of wild-type and *him-10*(RNAi) embryos. Shown are projections of confocal z-series through embryos stained with DAPI and hybridized with a probe to the 5S rDNA locus on chromosome V. (B) A wild-type embryo with uniformly diploid nuclei. (C) *him-10* RNAi embryo with a heterogeneous population of aneuploid nuclei. Sister nuclei (arrow) exhibiting 3–1 segregation are indicative of nondisjunction. (D) Scatter plot of the number of nuclei in an embryo (x axis) versus the number of nuclei in the mode of the embryo (y axis). The function $Y = (2C)^i$ is plotted for the *C* values indicated.

clei and mitotic structures (Fig. 3, B and E) compared with wild-type embryos (Fig. 3 A). Interphase nuclei were abnormally large or small (Fig. 3 B), probably due to aneuploidy and the formation of micronuclei (see below) rather than a defect in cytokinesis. Only bipolar spindles were observed (Fig. 3 B), rather than the multipolar spindles characteristic of cytokinesis defects (Kainta et al., 2000). At metaphase, chromosomes were often attached to only one spindle pole (Fig. 3, B and E, white arrow), and spindles were frequently bifurcated and bent—the chromatin was amassed on one side of the spindle midzone (Fig. 3, compare yellow arrows in A with those of B). Lagging and monooriented chromosomes were seen as early as anaphase of the first cell division. Spindles were typically elongated in metaphase and anaphase. These mutant phenotypes suggest a role for *him-10* in bipolar spindle attachment.

Multiple micronuclei, a feature typical of chromosome segregation mutants (Gonczy et al., 1999), were apparent in cells of *him-10*(RNAi) embryos (Fig. 3 G), but not those of wild-type embryos (Fig. 3 F). The multiple nuclei most likely resulted from the failure of lagging anaphase chromosomes to be incorporated into the main nucleus. In addition, *him-10*(RNAi) embryos exhibited an ingression of the cleavage furrow through lagging chromatin, thus producing a cut phenotype (Yanagida, 1998) in which two daughter nuclei were closely opposed (Fig 3 H). Analysis by EM confirmed that the nuclear envelope had formed around the independent or partially attached masses of chromatin within the same mutant cell (Fig. 3, I–K).

Despite having bifurcated spindles and chromosomes with unipolar attachments, the *him-10*–deficient embryos (Fig. 3 D) had a normal antibody staining pattern for the centromere-specific histone H3-like protein, HCP-3 (provided by M. Roth, Fred Hutchinson Cancer Research
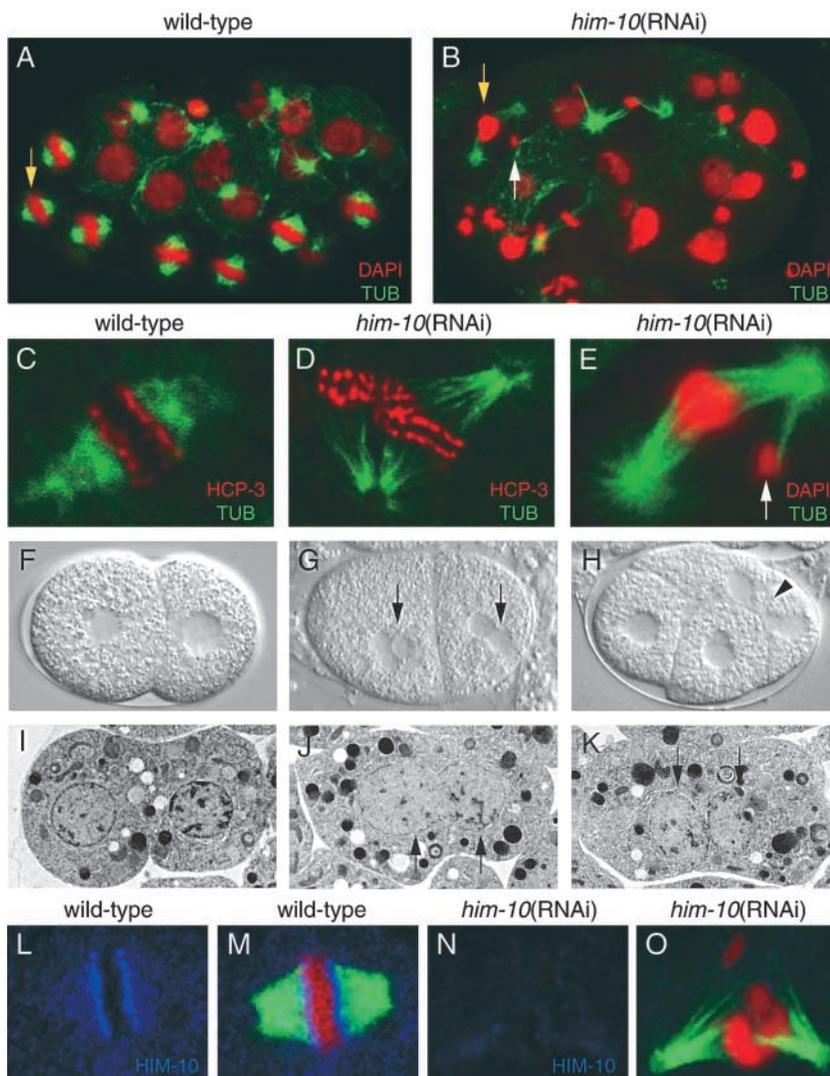
wild-type | **him-10(RNAi)**

wild-type | **him-10(RNAi)** | **him-10(RNAi)**

wild-type | **wild-type** | **him-10(RNAi)** | **him-10(RNAi)**

Figure 3. Depletion of HIM-10 causes defects in mitosis consistent with a failure in bipolar spindle attachment. (A and B) Projections of confocal z-series through embryos stained with DAPI (red) and antitubulin antibodies (green). (A) Wild-type embryo with several normal metaphase figures (yellow arrow). (B) An older *him-10*(RNAi) embryo with multiple defects in mitotic chromosome segregation consistent with a failure in bipolar spindle attachment. Interphase nuclei vary in size, indicating aneuploidy. Metaphase spindles are bent, bifurcated, and elongated; chromosomes attached to only one pole (white arrow and enlargement in E). (C and D) Single confocal sections through metaphase spindles of wild-type and *him-10*(RNAi) embryos costained with antitubulin (green) and anti–HCP-3 (red) antibodies. HCP-3 localizes to the poleward surfaces of metaphase chromatin in wild-type embryos (C). HCP-3 localizes normally to the microtubule-attached and unattached metaphase chromatids of *him-10*(RNAi) embryos (D). (F–H) Nomarski photomicrographs of wild-type (F) and *him-10*(RNAi) (G and H) embryos. Multinucleate cells (G, arrows) and cells showing ingression of the cleavage furrow through lagging chromatin (H, arrowhead) indicate defects in chromosome segregation. (I–K) Electron micrographs of interphase nuclei in HPF/FS prepared embryos. (I) Wild-type cell showing properly spaced and formed sister nuclei as the cytokinesis furrow initiates. (J) A single cell with a bilobed nucleus (arrows) from a *him-10*(RNAi) embryo. (K) A multinucleate (arrows) cell from a *him-10*(RNAi) embryo. (L–O) Mitotic figures of embryos costained with HIM-10 (blue), tubulin antibodies (green), and DAPI (red). In wild-type embryos (L and M), all chromosomes have established bipolar attachment and equatorial alignment on the metaphase plate. In *him-10*(RNAi) embryos HIM-10 signal is severely reduced on mitotic chromosomes (N and O). Some chromosomes failed to establish bipolar attachment and equatorial alignment.

Center, Seattle, WA) (Buchwitz et al., 1999; Fig. 3 C), implying that HIM-10 is not required for HCP-3 localization to centromeres. Thus, the nondisjunction of mitotic chromosomes in RNAi-treated embryos coupled with the cytologically aberrant mitotic structures suggests a role for HIM-10 in kinetochore function or microtubule dynamics.

HIM-10 Localizes to Kinetochore Regions of Mitotic Chromosomes

Confocal microscopy of animals stained with HIM-10 antibodies showed HIM-10 to be localized in a pattern expected for kinetochore proteins on holocentric chromosomes. Such chromosomes are distinguished by having their kinetochores and sites of microtubule attachment dispersed along the length of the chromosome. HIM-10 antibody staining was not detected on chromosomes of interphase nuclei. During prophase, HIM-10 was visualized as parallel tracks (in longitudinal sections) or paired dots (in cross sections) flanking each mitotic prophase chromosome (Fig. 4, A–G). At metaphase, HIM-10 was distributed in stripes along the poleward faces of the chromatin at the metaphase plate (Fig. 4, H–K). During anaphase, one poleward-facing stripe was associated with each set of sister chromatids (Fig. 4, L–O). Antibody staining was not detected during telophase. These staining patterns were most evident in the large cells of the early embryo but were also seen in the mitotic germline. HIM-10 antibody staining was not consistently seen on other structures in embryos or the mitotic germline, but a recurrent suggestion of spindle and centrosome staining was found with some antibody preparations. Both the specificity of the HIM-10 antibody and the dependence of the staining pattern on the presence of HIM-10 were confirmed by the severe reduction of HIM-10 antibody staining in *him-10*(RNAi) embryos (Fig. 3, N and O) compared with wild-type embryos (Fig. 3, L and M).

The HIM-10 staining pattern resembled the pattern of the *C. elegans* centromere-specific HCP-3 protein (Fig. 4, P–X) (Buchwitz et al., 1999), but two notable differences were apparent. HIM-10 was not detected in interphase nuclei where HCP-3 had a punctate pattern (data not shown), suggesting that HIM-10 assembles onto chromosomes af-
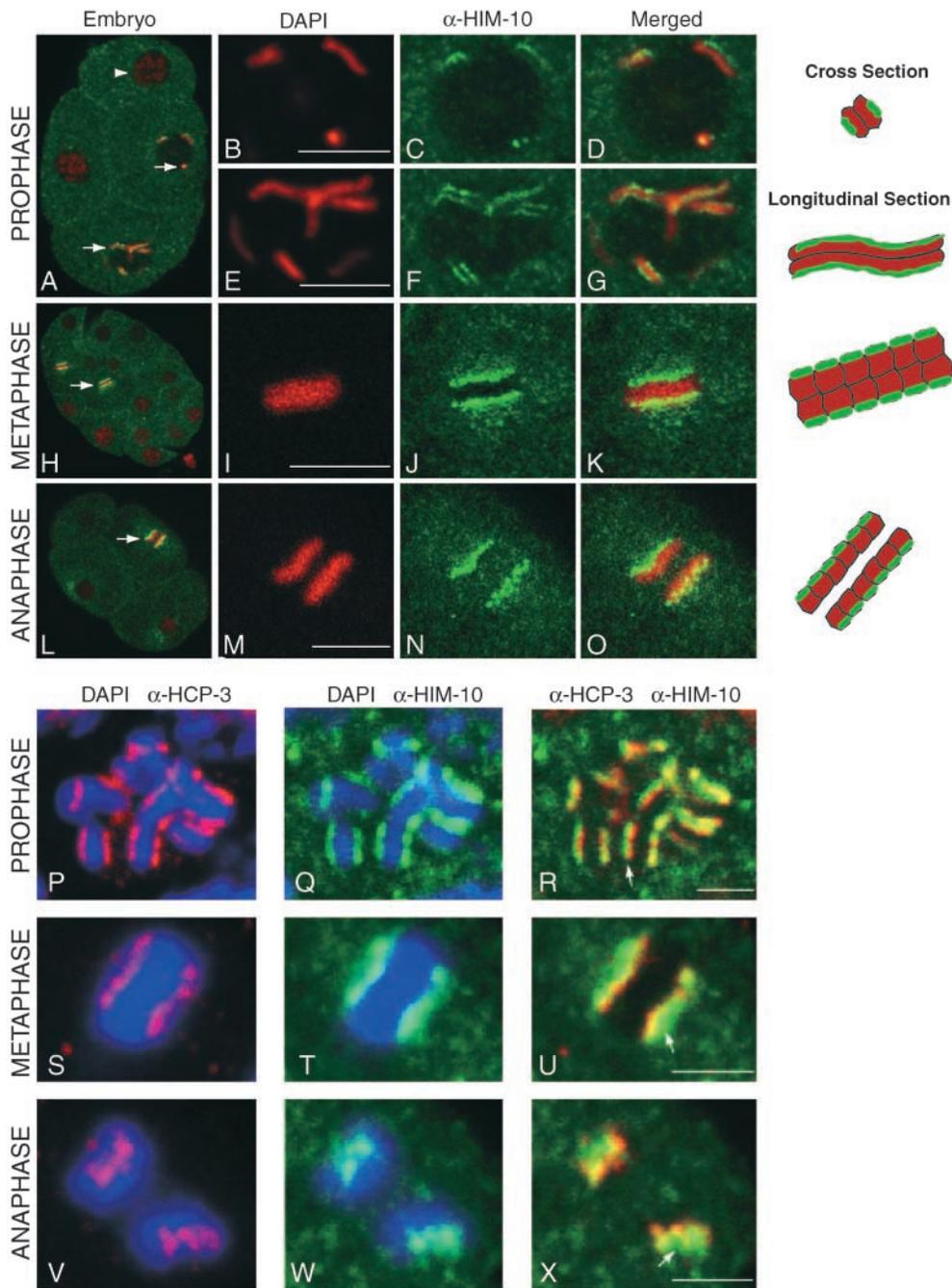
Figure 4. HIM-10 localizes to the kinetochore region of the kinetochore–centromere complex. All panels are false-color confocal images. Interpretative cartoons (right) represent images from D, G, K, and O. (A, H, and L) Wild-type embryos co-stained with DAPI (red) and anti-HIM-10 antibodies (green). (A) HIM-10 associates with prophase (arrows) but not interphase (arrowhead) chromosomes. (B–D) Enlargement of nucleus in A. In cross section, HIM-10 appears as paired dots flanking opposite sides of a prophase chromosome. (E–G) Enlargement of nucleus in A. HIM-10 forms two tracks flanking a prophase chromosome. (H) HIM-10 appears depleted from the cytoplasm of cells in metaphase. (I–K) Enlargement of metaphase cell (arrow) in H. HIM-10 appears as stripes associated with each poleward face of the metaphase plate. (L) An embryo with HIM-10 localized to the poleward face of anaphase chromosomes. (M–O) Enlargement of anaphase figure (arrow) in L. HIM-10 appears as many individual dots along the chromatin. These dots may represent the kinetochores associated with chromosomes moving at slightly different rates to the spindle pole. (P–X) Wild-type animals co-stained with DAPI (blue) and antibodies to both the centromeric marker HCP-3 (red) and HIM-10 (green). (P–R) Prophase nucleus from the mitotic region of the hermaphrodite gonad. (P and Q) Both proteins localize in two parallel tracks flanking the replicated chromosomes. (R) The HIM-10 signal overlaps with (yellow) and extends more distal to (green) the HCP-3 signal. In metaphase (S–U) and anaphase (V–X) of embryos, both proteins localize to the poleward face of the chromatin. In the merged images (U and X) HIM-10 overlaps with (yellow) and extends closer to the pole than (green) HCP-3. Bars, 2 μm.

ter HCP-3. HIM-10 was closer to the pole than HCP-3 from prophase through anaphase (Fig. 4, R, U, and X), implying a role for HIM-10 in a kinetochore function such as spindle attachment, rather than a centromere function.

The Kinetochore Structure Visualized by EM Is Disrupted in him-10(RNAi) Embryos

Conventional EM showed that the metaphase kinetochore of *C. elegans* is a convex plaque that covers the entire pole-

ward face of chromosomes. It has a trilaminar structure composed of electron-dense inner and outer layers with an electron lucent middle layer (Albertson and Thomson, 1982), indicating that the holocentric *C. elegans* kinetochore is an extended version of a conventional kinetochore (Roos, 1973; Albertson and Thomson, 1982). To understand the function of HIM-10 within the kinetochore, we analyzed metaphase chromosomes of wild-type and HIM-10–depleted embryos prepared for EM using a pro-

cedure optimized for preservation of structure: HPF followed by FS (McDonald, 1999; Rappleye et al., 1999).

In serial sections of electron micrographs from wild-type embryos, a different morphology for the holocentric *C. elegans* kinetochore was observed from that reported using conventional EM. Instead of a trilaminar structure, a clear zone that excludes ribosomes and other cytoplasmic components was found along each poleward face of wild-type metaphase chromatin. (Fig. 5 A, black arrow). In some sections, a line of light-staining material (Fig. 5 C, white arrow) was apparent between the clear zone and the chromatin, suggestive of a structural element adjacent to the chromatin on the metaphase plate. The position of the clearing and light-staining material at the interface of the chromatin and the spindle microtubules suggests that these features are associated with the kinetochore or a structure within the kinetochore.

Rat kangaroo cells prepared with HFP/FS revealed a similar kinetochore structure (McEwen et al., 1998). The authors argued that the trilaminar structure defined by conventional EM was a consequence of solvent-mediated shrinking and precipitation that does not occur with HFP/FS. Instead of a trilaminar structure, the monocentric kinetochores of the vertebrate cells have a thick mat of light-staining fibrous material that is connected to the centromeric heterochromatin. The fibrous mat corresponds to the outer plate defined by conventional EM, where the spindle microtubules terminate. This mat is surrounded on its cytoplasmic surface by a clear zone that excludes ribosomes, a zone that correlates with the fibrous corona seen in conventional EM preparations. The fibrous mat and the ribosome-free zone of the vertebrate kinetochore are reminiscent, respectively, of the light-staining structural element and the clear zone seen in *C. elegans*, further suggesting that these features define the *C. elegans* kinetochore.

We examined the microtubule plus ends in the vicinity of the chromatin to determine the distribution of their ends relative to the ribosome-free zone. A heterogeneous picture emerged. Some microtubules ended before reaching the chromatin, possibly in the fibrous material (Fig. 5 E, small arrow). Some microtubules extended all the way to the chromatin (Fig. 5 E, arrowhead), and other microtubules appeared to penetrate the chromatin (Fig. 5 E, arrow), probably passing between adjacent chromosomes. The ribosome-free zone was difficult to identify in the thin sections required to detect microtubules, a finding consistent with the observations of McEwen et al. (1998) who also found that wherever microtubules were bound to chromatin, the ribosome-free zone was difficult to observe. Quantitative analysis by tomography or perhaps serial sections will be required to understand the high resolution structure of this boundary.

Depletion of HIM-10 disrupted this kinetochore structure. In *him-10* RNAi embryos, the clear zone was greatly diminished or not evident along the metaphase chromatin (Fig. 5, B and D), suggesting that HIM-10 protein is necessary for the proper formation and function of the *C. elegans* kinetochore.

Serial section EM analysis also confirmed the aberrant mitotic structures in HIM-10–depleted embryos—bent and elongated spindles—seen by light microscopy. Chromatin of the wild-type metaphase spindle (Fig. 5 A) was positioned directly between the spindle poles. By contrast, chromatin of *him-10* RNAi embryos (Fig. 5 B) was amassed on one side of the spindle midzone, and the spindles were elongated compared with those in wild-type embryos.

Kinetochore Structure and HIM-10 Localization on Meiotic Chromosomes

EM analysis of chromosomes from spermatocytes (Fig. 5 F) in metaphase of meiosis also revealed a zone of ribosome exclusion surrounding the homologous chromosomes (large arrow), suggesting that meiotic chromosomes have a kinetochore structure similar to that of mitotic chromosomes. A higher magnification view of the ribosome-free zone in a male meiotic spindle (Fig 5, inset) shows microtubules in cross section, an orientation parallel to the chromatin surface. This orientation is in contrast to the mostly perpendicular orientation of the microtubules in the mitotic spindles.

Conventional EM had failed to show the trilaminar kinetochore structure on *C. elegans* meiotic chromosomes (Albertson and Thomson, 1993). Spindles were thought to attach directly to the chromatin. The similarities in mitotic and meiotic chromosome structure apparent through the use of HFP/FS suggest that mitotic kinetochore proteins may also play a role in the segregation of holocentric meiotic chromosomes.

Using confocal microscopy, we found that HIM-10 surrounds the chromosomes of spermatocytes and fertilized eggs in metaphase I, as does the ribosome-free zone, indicating a shared molecular component between meiotic and mitotic kinetochores. HIM-10 staining is absent from pachytene nuclei in both males and hermaphrodites. HIM-10 accumulates on the bivalents in ooctye diakinesis, encasing them, as shown by the combination of cross sections and grazing sections (Fig. 6 A). The HIM-10 coat remains on the chromosomes in prometaphase of meiosis I (Fig. 6 C) and meiosis II (not shown). In prometaphase of meiosis I, HIM-10 staining (Fig. 6 K) surrounds HCP-3 (Fig. 6 J) and DAPI (Fig. 6 I) staining of the bivalents. In males, HIM-10 is absent from most, if not all, stages of meiotic prophase. HIM-10 then encases metaphase I (Fig. 6, E and F), anaphase I (Fig. 6 G), and metaphase II chromosomes of spermatocytes.

We also found that HIM-10 encases both extrachromosomal DNA arrays (Fig. 6 B, green arrow) and free chromosomal duplications (not shown) during female meiosis. Just as in mitosis, arrays and duplications can segregate during meiosis, but with reduced efficiency compared with whole chromosomes. Since arrays and duplications are difficult to identify during mitosis, we extrapolate from the staining pattern in meiosis that HIM-10 also localizes to arrays and duplications during mitosis. Loss of HIM-10 activity would therefore be likely to decrease the attachment of spindles to free duplications and thereby account for their decrease in mitotic stability in *him-10* mutants.

The discovery that meiotic chromosomes are surrounded by both the ribosome-free zone and HIM-10 protein suggested the functional similarity in microtubule–chromosome interactions during meiosis and mitosis in an organism with holocentric chromosomes. To understand further how meiotic chromosomes attach to spindles, we asked whether reduction of *him-10* activity affects meiotic chromosome segregation.
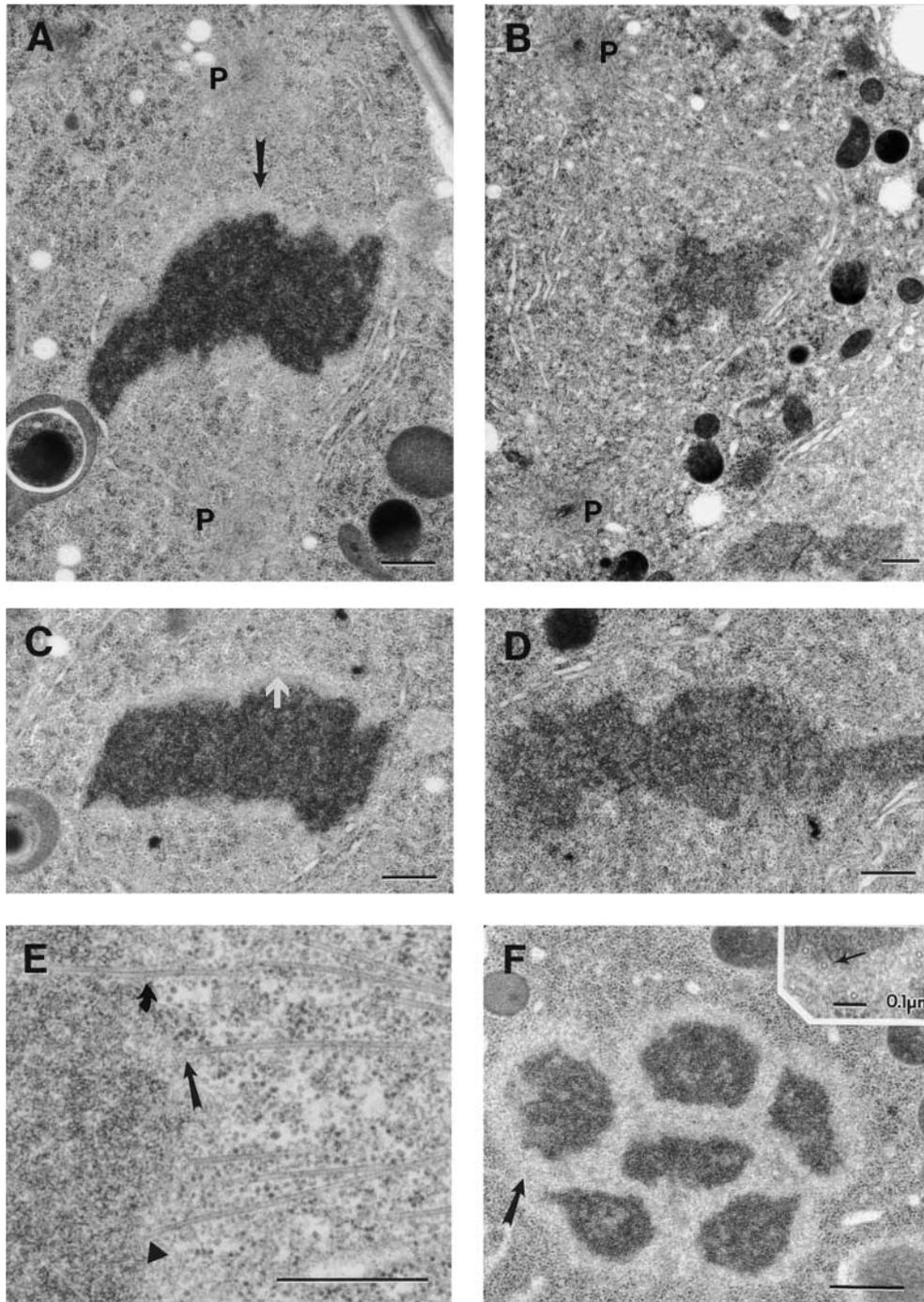
Figure 5. Depletion of HIM-10 disrupts the morphology of the mitotic kinetochore. (A–F) Electron micrographs of samples prepared by HPF followed by FS. (A) Medial longitudinal section through the metaphase plate of a wild-type embryo. Poles are marked (P), the electron dense chromatin is aligned directly between poles, and the nuclear envelope is partially intact. A ribosome-free zone (arrow) is associated with each poleward face of the chromatin. (B) Medial longitudinal section through the metaphase plate of a *him-10*(RNAi) embryo. Centrioles are evident at both spindle poles, the chromatin is amassed on one side of the spindle midzone, and the ribosome-free zone is greatly diminished or absent. The spindles are elongated compared with those in A. (C) Longitudinal section through the wild-type metaphase plate seen in A. Light-staining fibrous element (white arrow) lies at the surface of the chromatin, and the ribosome-free zone extends poleward from the fibrous element. (D) Longitudinal section through a metaphase plate from the *him-10*(RNAi) embryo in B. The ribosome-free zone is severely diminished. (E) High magnification view of a wild-type metaphase spindle in longitudinal section showing microtubules ending in the chromatin (arrowhead) and in material on the face of the chromatin (arrow). Microtubules passing between chromosomes are also seen (curved arrow). (F) A cross section through the spindle equator of a wild-type spermatocyte in metaphase I of meiosis. A wide ribosome-free halo (large arrow) is evident surrounding the chromatin. A higher magnification view of the ribosome-free zone (inset) shows microtubules in cross section (arrow), indicating an orientation in parallel to the surface of the chromatin. Bars, 0.5 μm, except as noted in inset.

Meiotic Chromosome Segregation Is Disrupted in Animals with Reduced him-10 Activity

A specific temperature-shift regime with *him-10*(*e1511*ts) hermaphrodites allowed us to disrupt meiotic chromosome segregation without affecting mitotic chromosome segregation. We had noticed a dramatic reduction in the brood size of *him-10*(ts) hermaphrodites raised at the restrictive temperature during the L4 larval stage, when sperm meiosis occurs, but not during other larval stages. We therefore shifted wild-type and *him-10* mutant L4s to the restrictive temperature and assessed meiotic chromosome segregation defects using FISH analysis with a 5S rDNA probe. As with the previous FISH analysis, the copy number of chromosome V was determined for all nuclei in an embryo, and for each embryo, a mode was determined that reflected the most frequent class of nuclei within the embryo. A defect in meiosis but not mitosis is
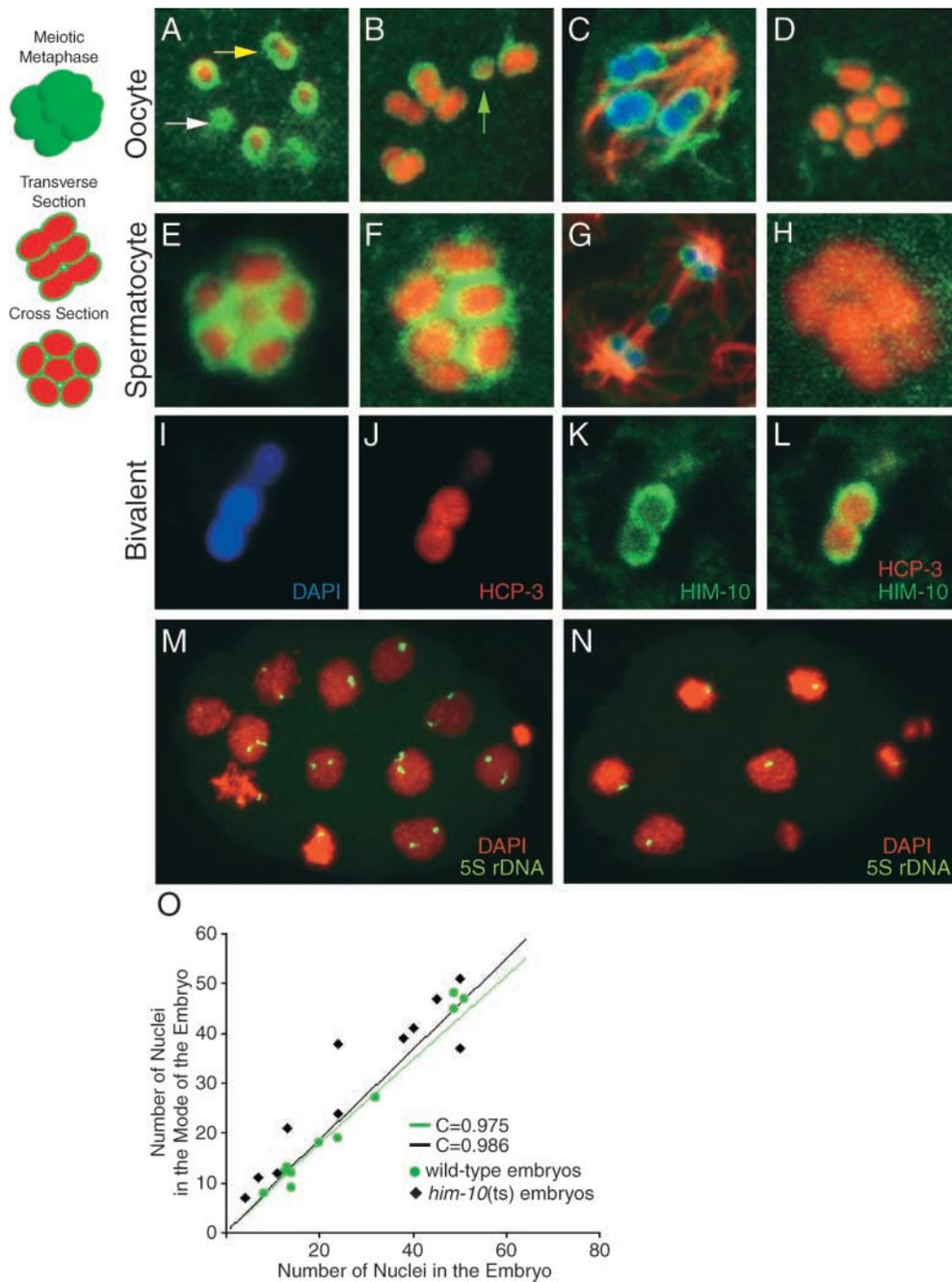
Figure 6. HIM-10 localizes to meiotic chromosomes and is required for meiotic chromosome segregation. All panels are false-color confocal images. Interpretative cartoons (left) depict meiotic chromosomes (red) labeled with HIM-10 antibody (green). (A–H) Oocytes or eggs (in hermaphrodites) and spermatocytes (in males) stained with HIM-10 antibody (green) and DAPI (red, except blue in C and G). (A) A wild-type oocyte in diakinesis. In a grazing section (white arrow), HIM-10 appears to coat the chromosome. In a cross section (yellow arrow), HIM-10 appears as a halo around the chromosome. (B) An oocyte in diakinesis. HIM-10 surrounds all six bivalents and the one extrachromosomal array (green arrow). (C) Transverse section through a wild-type egg in meiotic prometaphase also stained with DAPI (blue) and antitubulin antibody (red). HIM-10 encases the bivalents and seems to associate with some spindle microtubules. (D) Cross section through the metaphase plate of an egg in a *him-10*(ts) mutant hermaphrodite raised at 25°C. The HIM-10 signal appears as a halo around the chromosomes, indicating that the protein was present. (E) A cross section and a superficial transverse section (F) through the chromatin of a wild-type spermatocyte in metaphase I. HIM-10 protein forms a halo around the chromosomes. (G) Transverse section through a wild-type spermatocyte in anaphase I stained with DAPI (blue) and antibodies to tubulin (red) and HIM-10 (green). The X chromosome is a univalent and lags at the spindle equator as the halves of the autosomal bivalents arrive at the spindle poles. (H) A transverse section through the metaphase plate of a *him-10*(ts) male raised at 25°C. The HIM-10 signal is greatly reduced. (I–L) A transverse section through a bivalent in prometaphase of meiosis I from an egg costained with DAPI (I), anti-HCP-3 (J), and anti-HIM-10 (K). L is a merged image of J and K. (M–N) FISH analysis of wild-type and *him-10*(ts) embryos. Shown are projections of confocal z-series through embryos stained with DAPI and hybridized with a probe to the 5S rDNA locus on chromosome V. (M) An embryo from a wild-type hermaphrodite shifted to 25°C at L4. The embryo is diploid. (N) An embryo from a *him-10*(ts) mutant hermaphrodite shifted to 25°C at L4. The embryo is monosomic for chromosome V. (O) Scatter plot of the number of nuclei in an embryo (x axis) versus the number of nuclei in the mode of the embryo (y axis). The function $Y = (2C)^i$ is plotted for the C values indicated.

expected to result in embryos with a homogeneous population of nuclei in a mode other than two (Figs. 2 A and 6 N). In our control experiment, 10 of 11 wild-type embryos had a mode of two and a homogeneous population of nuclei (Fig. 6 M). By contrast, only 4 of 12 embryos from temperature-shifted mothers had a mode of two, whereas six had a mode of one (Fig. 6 N), and two had a mode of three. All 12 embryos had a homogeneous population of nuclei. Therefore, 8 of 12 embryos from temperature-shifted mothers (compared with 1 of 11 control embryos, $P = 0.009$) exhibited aberrant segregation of chromosome V during meiosis. Consistent with a selective disruption of

spermatocyte meiosis, HIM-10 staining was significantly reduced on chromosomes of spermatocytes (Fig. 6 H), but not those of fertilized eggs (Fig. 6 D), in animals treated with the temperature-shift regime described above.

The conclusion, that meiotic but not mitotic chromosome segregation was disrupted by temperature shift at L4, was reinforced by quantitative analysis showing that the probability (C) of proper chromosome V segregation during the mitotic cell divisions of *him-10*(ts) embryos ($C = 0.99$) was statistically indistinguishable from that of wild type ($C = 0.98$), indicating that normal mitotic chromosome segregation had occurred in the mutant embryos (Fig. 6 O). These data provide the first evidence that a protein with essential kinetochore function during mitosis is also critical for proper chromosome segregation during meiosis in an organism with holocentric chromosomes.

Discussion

We have shown that HIM-10 is a component of the kinetochore that is essential for the segregation of *C. elegans* holocentric chromosomes during mitosis and meiosis. HIM-10 is related to the Nuf2 kinetochore proteins conserved from yeast to humans (Wigge and Kilmartin, 2001), indicating that kinetochore components are conserved between monocentric and holocentric chromosomes. Depletion of HIM-10 caused a failure of bipolar spindle attachment, lagging anaphase chromosomes, and sister chromatid nondisjunction—all defects consistent with a role for HIM-10 in mediating attachment of chromosomes to the mitotic spindle, a conclusion not demonstrated by previous work on Nuf2. The structure of the *C. elegans* mitotic kinetochore determined by EM analysis resembles that of the vertebrate kinetochore and is disrupted by depletion of HIM-10, indicating that HIM-10 is necessary for the proper assembly and function of the kinetochore. A structure resembling the mitotic kinetochore was also found encircling the *C. elegans* meiotic chromosomes. Correlating with the location of this structure, HIM-10 encases the meiotic chromosomes, and reduction of HIM-10 function causes disruption of meiotic chromosome segregation. These findings show that meiotic chromosomes in an organism with holocentric chromosomes possess kinetochores that share molecular, morphological, and functional features with those of mitotic chromosomes. Consistent with the holocentric nature of worm kinetochores, HIM-10 surrounds free chromosomal duplications. Even foreign DNA, organized into extra chromosome arrays, assembles worm kinetochores.

Role of HIM-10 in Kinetochore Structure and Function

The change in kinetochore morphology in response to HIM-10 depletion raises several possibilities for the role of HIM-10 in kinetochore structure and function. HIM-10 might be a component of the fibrous mat and mediate formation of the ribosome-free zone by its localization and function within the mat. In this capacity, HIM-10 could act early to recruit additional components of the kinetochore that are essential for its structure and function. Alternatively, HIM-10 could localize to the ribosome-free zone and facilitate its formation. In this case, HIM-10 could act later in the assembly process, for example, to tether a motor protein.

As a coiled coil protein, HIM-10 is well suited for either role. Coiled coils are excellent oligomerization domains and function commonly in the assembly of protein complexes. Of direct relevance, the coiled coils of *S. cerevisiae* Nuf2 have been shown to interact broadly in the yeast two-hybrid assay with the coiled coils of many chromosome segregation proteins, including mitotic kinesins and cytoplasmic dynein (Newman et al., 2000).

Chromosome–microtubule attachment is of such fundamental importance that one might expect considerable redundancy in the mechanisms establishing and maintaining bipolar spindle attachment. In this light, it is perhaps of no surprise that depletion of HIM-10 does not completely abolish bipolar alignment. A similar phenomenon was found in connection with the depletion from human cells of CENP-E, a kinetochore motor required for metaphase chromosome attachment and alignment (Yao et al., 2000).

Kinetochore Activity on C. elegans Meiotic Chromosomes

Evidence for a kinetochore on holocentric chromosomes in meiosis had been lacking. A trilaminar structure had not been observed (Albertson and Thomson, 1993). Although the novel mitotic kinetochore protein HCP-1 surrounds meiotic chromosomes, a role for HCP-1 in meiosis had not been established (Moore et al., 1999). Our EM studies have now revealed a ribosome-free zone surrounding meiotic chromosomes that is reminiscent of the ribosome exclusion zone on mitotic chromosomes of *C. elegans* and mammalian cells. Moreover, the essential mitotic kinetochore protein, HIM-10, surrounds *C. elegans* meiotic chromosomes and is necessary for their segregation. Together, these results show that HIM-10 contributes to kinetochore activity during meiosis. Thus, in an organism with holocentric chromosomes, chromosome–microtubule interactions in meiosis have structural and functional similarities with those in mitosis.

The fact that HIM-10 protein is not restricted to the poleward regions of meiotic bivalents, as it is on mitotic chromosomes, raises interesting questions about microtubule attachment and chromosome alignment during meiosis. Both conventional EM and HFP/FS procedures showed abundant microtubules running laterally along the surfaces of the axially oriented bivalents at metaphase. Do these lateral microtubules attach to the chromatin and contribute to alignment during metaphase and segregation during anaphase? Microtubules might attach to both lateral and poleward surfaces of chromosomes, consistent with the location of HIM-10, provided that microtubules from one pole attach to only one homologue. The possibility also exists that microtubules attach only to the poleward ends of the chromosomes. This could be accomplished by limiting access to HIM-10 or by damping HIM-10 activity on lateral surfaces. Alternatively, HIM-10 could interact with proteins only on poleward ends to promote microtubule attachment and kinetochore activity. By either mechanism, HIM-10 would be necessary but not sufficient for correct spindle attachment.

The findings presented here highlight the utility of *C. elegans* in dissecting kinetochore structure and function in both mitosis and meiosis. The underlying molecular and structural similarities between worm and mammalian ki-

netochores, coupled with the ease in analyzing chromosomes, make *C. elegans* a powerful guide for the molecular dissection of the mammalian kinetochore.

References

Albertson, D.G., and J.N. Thomson. 1982. The kinetochores of *Caenorhabditis elegans*. *Chromosoma*. 86:409–428.

Albertson, D.G., and J.N. Thomson. 1993. Segregation of holocentric chromosomes at meiosis in the nematode, *Caenorhabditis elegans*. *Chromosome Res*. 1:15–26.

Albertson, D.G., A.M. Rose, and A.M. Villeneuve. 1997. Chromosome Organization, Mitosis and Meiosis. *In C. elegans* II. D.L. Riddle, T. Blumenthal, B. J. Meyer, and J.R. Priess, editors. Cold Spring Harbor Laboratory Press, Cold Spring Harbor, NY. 47–78.

Amon, A. 1999. The spindle checkpoint. *Curr. Opin. Genet. Dev*. 9:69–75.

Buchwitz, B.J., K. Ahmad, L.L. Moore, M.B. Roth, and S. Henikoff. 1999. A histone-H3-like protein in *C. elegans*. *Nature*. 401:547–548.

Dernburg, A.F., and J.W. Sedat. 1998. Mapping three-dimensional chromosome architecture in situ. *Methods Cell Biol*. 53:187–233.

Fire, A., S.-Q. Xu, M.K. Montgomery, S.A. Kostas, S.E. Driver, and C.C. Mello. 1998. Potent and specific genetic interference by double-stranded RNA in *Caenorhabditis elegans*. *Nature*. 391:806–810.

Gonczy, P., H. Schnabel, T. Kaletta, A.D. Amores, T. Hyman, and R. Schnabel. 1999. Dissection of cell division processes in the one cell stage *Caenorhabditis elegans* embryo by mutational analysis. *J. Cell Biol*. 144:927–946.

Harlow, E., and D. Lane. 1988. Antibodies, A Laboratory Manual. Cold Spring Harbor Laboratory Press, Cold Spring Harbor, NY. 353–356.

Heald, R. 2000. Motor function in the mitotic spindle. *Cell*. 102:399–402.

Hedgecock, E.M., and R.K. Herman. 1995. The *ncl-1* gene and genetic mosaics of *Caenorhabditis elegans*. *Genetics*. 141:989–1006.

Hodgkin, J., H.R. Horvitz, and S. Brenner. 1979. Non-disjunction mutants of the nematode *Caenorhabditis elegans*. *Genetics*. 91:67–94.

Howman, E.V., K.J. Fowler, J.N. Ainsley, S. Redward, A.C. MacDonald, P. Kalitsis, and K.H.A. Choo. 2000. Early disruption of centromeric chromatin organization in centromere protein A (*Cenpa*) null mice. *Proc. Natl. Acad. Sci. USA*. 97:1148–1153.

Kainta, S., M. Mendoza, V. Jantsch-Plunger, and M. Glotzer. 2000. Incenp and an Aurora-like kinase form a complex essential for chromosome segregation and efficient completion of cytokinesis. *Curr. Biol*. 10:1172–1181.

Kimble, J.E., and J.G. White. 1981. On the control of germ cell development in *Caenorhabditis elegans*. *Dev. Biol*. 81:208–219.

Lombillo, V.A., C. Nislow, T.J. Yen, V.I. Gelfand, and J.R. McIntosh. 1995. Antibodies to the kinesin motor domain and CENP-E inhibit microtubule depolymerization-dependent motion of chromosomes in vitro. *J. Cell Biol*. 128:107–115.

Maney, T., L.M. Ginkel, A.W. Hunter, and L. Worderman. 2000. The kinetochore of higher eukaryotes: a molecular view. *Int. Rev. Cytol*. 194:67–131.

McDonald, K.L. 1999. High pressure freezing for preservation of high resolution fine structure and antigenicity for immunolabeling. *Methods Mol. Biol*. 117:77–97.

McEwen, B.F., C. Hsieh, A.L. Matteyses, and C.L. Rieder. 1998. A new look at kinetochore structure in vertebrate somatic cells using high-pressure freezing and freeze-substitutions. *Chromosoma*. 107:366–375.

Mello, C., and A. Fire. 1995. DNA transformation. *Methods Cell Biol*. 48:451–482.

Moore, L.L., M. Morrison, and M.B. Roth. 1999. HCP-1, a protein involved in chromosome segregation, is localized to the centromere of mitotic chromosomes in *Caenorhabditis elegans*. *J. Cell Biol*. 147:471–479.

Nabetani, A., T. Koujin, C. Tsutsumi, T. Haraguchi, and Y. Hiraoka. 2001. A conserved protein Nuf2 is implicated in connecting the centromere to the spindle during chromosome segregation: a link between the kinetochore function and the spindle checkpoint. *Chromosoma*. In press.

Newman, J.R.S., E. Wolf, and P.S. Kim. 2000. A computationally directed screen identifying interacting coiled coils from *Saccharomyces cerevisiae*. *Proc. Nat. Acad. Sci. USA*. 97:13203–13208.

Nicklas, R.B. 1997. How cells get the right chromosomes. *Science*. 275:632–637.

O'Connell, K.F., C.M. Leys, and J.G. White. 1998. A genetic screen for temperature-sensitive cell-division mutants of *Caenorhabditis elegans*. *Genetics*. 149:1303–1321.

Rappleye, C.A., A.R. Paredez, C.W. Smith, K.L. McDonald, and R.V. Aroian. 1999. The coronin-like protein POD-1 is required for anterior-posterior axis formation and cellular architecture in the nematode *Caenorhabditis elegans*. *Genes Dev*. 13:2838–2851.

Roos, U.-P. 1973. Light and electron microscopy of rat kangaroo cells in mitosis. II. Kinetochore structure and function. *Chromosoma*. 41:195–220.

Savoian, M.S., M.L. Goldberg, and C.L. Rieder. 2000. The rate of chromosome poleward motion is attenuated in *Drosophila zw10* and *rod* mutants. *Nat. Cell Biol*. 2:948–952.

Shah, J.V., and D.W. Cleveland. 2000. Waiting for anaphase: Mad2 and the spindle assembly checkpoint. *Cell*. 103:997–1000.

Sharp, D.J., G.C. Rogers, and J.M. Scholey. 2000a. Cytoplasmic dynein is required for poleward chromosome movement during mitosis in *Drosophila* early embryos. *Nat. Cell Biol*. 2:922–930.

Sharp, D.J., G.C. Rogers, and J.M. Scholey. 2000b. Microtubule motors in mitosis. *Nature*. 407:41–47.

Wigge, P.A., and J.V. Kilmartin. 2001. The Ndc80p complex from *Saccharomyces cerevisiae* contains conserved centromere components and has a function in chromosome segregation. *J. Cell Biol*. 152:349–360.

Yanagida, M. 1998. Fission yeast cut mutation revisited: control of anaphase. *Trends Cell Biol*. 8:144–149.

Yao, X., A. Abrieu, Y. Zheng, K.F. Sullivan, and D.W. Cleveland. 2000. CENP-E forms a link between attachment of spindle microtubules to kinetochores and the mitotic checkpoint. *Nat. Cell Biol*. 2:484–491.